Encapsulation of the Antimicrobial and Immunomodulator Agent Nitazoxanide Within Polymeric Micelles

Romina J. Glisoni[1, 2] and Alejandro Sosnik[1, 2, *]

[1] *The Group of Biomaterials and Nanotechnology for Improved Medicines (BIONIMED),*
Department of Pharmaceutical Technology, Faculty of Pharmacy and Biochemistry,
University of Buenos Aires, Buenos Aires CP1113, Argentina
[2] *National Science Research Council (CONICET), Buenos Aires, Argentina*

Nitazoxanide (NTZ) is a highly hydrophobic nitrothiazolyl-salicylamide that displays antimicrobial activity against a variety of parasites, anaerobic bacteria and viruses. More recently, its effectiveness in the pharmacotherapy of chronic hepatitis, the leading cause of liver cirrhosis and hepatocellular carcinoma (HCC), has been reported. On the other hand, the extremely low aqueous solubility of the drug challenges its administration by different routes. The present work explored for the first time the encapsulation of NTZ within pristine, lactosylated and mixed poly(ethylene oxide)–poly(propylene oxide) (PEO–PPO) polymeric micelles (PMs) of different architectures, molecular weights and hydrophilic-lipophilic balance (HLB) as a strategy to improve its aqueous solubility and to potentially target it to the liver parenchyma. The solubility was increased up to 609 times. The drug encapsulation modified the self-aggregation pattern of the different amphiphiles, resulting in a sharp growth of the micellar size. The encapsulation capacity of the lactosylated derivatives was smaller than that of the pristine counterparts, though the development of mixed PMs that combine a highly hydrophilic lactosylated amphiphile (e.g., poloxamer F127 or poloxamine T1107) that forms the micellar template and a more hydrophobic unmodified poloxamine (T904) that increases the hydrophobicity of the core resulted in the synergistic encapsulation of the drug and a substantial increase of the physical stability over time. Overall findings confirmed the extremely great versatility of the poloxamer/poloxamine mixed self-assembly systems as Trojan nanocarriers for the encapsulation of NTZ towards its targeting to the liver.

Keywords: Nitazoxanide, Viral Hepatitis, Polymeric Micelles, Lactosylated Nanocarriers.

RESEARCH ARTICLE

1. INTRODUCTION

Hepatitis B and C are unique infectious diseases because of the prodigious capacity of both viruses to cause persistent infection of the human liver, cirrhosis and hepatocellular carcinoma (HCC).[1] HCC is one of the most common and lethal malignant tumors in the word,[2] chronic hepatitis being responsible for the great majority of cases of HCC.[3] Approximately 695,000 people die due to HCC every year.[4,5] Current standard therapies for both chronic infections have a relatively low effectiveness. Thus, the search for new antiviral agents is an urgent need.[6–9] At the same time, the development of innovative drug delivery systems (DDS) that make possible their selective accumulation in the hepatic parenchyma would contribute to improve the efficacy of drugs already approved by the regulatory agencies.[10]

Nitazoxanide (NTZ; [2-[5-nitro-1,3-thiazol-2-yl)carbamoyl]phenyl] acetate), a poorly water-soluble thiazolide derivative, was first licensed in the USA for the treatment of diarrhea and enteritis caused by infections of *Cryptosporidium parvum* and *Giardia lamblia* in adults and children above one year of age.[11,12] In addition to its proven antiprotozoal activity, it has been consistently shown that NTZ displays activity against a broad spectrum of helminths,[13–15] bacteria[16–18] and DNA/RNA viruses.[19,20] In this regard, it was recently discovered that NTZ and other thiazolides are effective against viral hepatitis.[21,22] Phase II clinical trials have demonstrated the efficacy and safety of NTZ when combined with PEGylated interferon (with or without ribavirin) in treating patients with chronic hepatitis C.[23] More limited clinical data indicated

*Author to whom correspondence should be addressed.

the potential activity of NTZ in chronic hepatitis B.[21] NTZ also showed synergistic antiviral effect in combination with other antivirals such as lamivudine or adefovir.[24] The antiviral activity of NTZ has been ascribed to its strong immunomodulatory effect[25] that includes an increase in IFNg- and IL2-secreting CD4+ T cells, cytotoxic T lymphocyte degranulation, Fas-expressing CD8+ T cells, TLR8-expressing monocytes, IFNa- and IFNb- mRNA expression, mRNA specific for type I IFN inducible genes mRNA specific for genes involved in MHC class I presentation.[26] Even though, NTZ shows a very favorable toxicity profile,[27] its relatively high melting temperature ($T_m = 202$ °C) and poor aqueous solubility (~7 μg/mL) might preclude the ability to develop pharmaceutical products with appropriate biopharmaceutic performance.

Encapsulation of hydrophobic drug molecules within polymeric micelles (PMs) represents one of the most versatile nanotechnology tools to enhance the aqueous solubility of poorly-water soluble drugs.[28–30] PMs are nanoscopic structures formed by the self-association of amphiphilic polymeric molecules in water above the critical micellar concentration (CMC).[28, 29] Due to the hydrophobicity of the core, these structures suit for the encapsulation, physicochemical stabilization and release of hydrophobic drugs.[28–30]

The thermo-responsive poly(ethylene oxide)-poly(propylene oxide) (PEO–PPO) block copolymers are among the most popular self-assembly biomaterials.[31, 32] Poloxamers are PEO–PPO-PEO triblocks, while poloxamines are four-armed derivatives. The latter present a central ethylendiamine residue that confers the amphiphile dependency to pH.[33] Owing to the broad spectrum of molecular features, these copolymers have been investigated in the encapsulation, release and targeting of different drugs.[34–36] In addition, the good biocompatibility enabled the administration by various routes such as oral, intravenous, ocular and intranasal.[35–39] Moreover, some of these amphiphiles downregulate the expression and inhibit the functional activity of efflux pumps of the ATP-binding cassette (ABC) superfamily in cancer and liver cell lines,[40–42] becoming attractive "Generally Regarded As Safe" (GRAS) nano-pharmaceuticals.[43]

Active targeting of antiviral agents to the infected liver parenchyma relies on the selective recognition and uptake of the drug-loaded delivery system by receptors present on the surface of the hepatocyte. This approach may increase the effectiveness of the therapy, while decreasing the systemic exposure and the potential side effects of drugs in non-target organs.[6]

Each hepatocyte displays between 50,000 to 500,000 asialoglycoprotein receptors (ASGPR).[44] Due to their capacity to internalize galactosylated molecules and particles, ASGPR represent an appealing pathway to improve the delivery of antiviral drugs to the liver parenchyma.[45–48]

In a recent work, we synthesized and fully characterized the physicochemical and self-aggregation properties of lactosylated PEO–PPO poloxamers and poloxamines and showed the agglutination of the modified PMs with a soluble lectin *in vitro*.[49]

The present work reports for the first time on the nanoencapsulation of NTZ. The capacity of different pristine and lactosylated single and mixed PEO–PPO PMs was assessed. Pristine and lactosylated mixed F127:T904 and T1107:T904 PMs took advantage of the greater encapsulation capacity of poloxamine T904 and the better physical stability of F127 and T1107 micelles.

2. MATERIALS AND METHODS

2.1. Materials

Poloxamer Pluronic® F127 (MW 12.6 kg/mol, 70 wt% PEO, HLB 18-23) and poloxamines Tetronic® 1107 (T1107, MW 15 kg/mol, 70 wt% PEO, HLB 18–23) and 904 (T904, MW 6.7 kg/mol, 40 wt% PEO, HLB 12–18) were a gift of BASF Corporation (New Milford CT, USA). Lactobionic acid (LA, technical grade 97%), N,N'-dicyclohexylcarbodiimide (DCC) and 4-dimethylaminopyridine (DMAP) were purchased from Sigma-Aldrich (St. Louis, MO, USA) and used as received. Nitazoxanide (NTZ, Fig. 1) was isolated from commercially available Nixoran® tablets (500 mg, Laboratorios Roemmers, Argentina) and purified by recrystallization from ethyl acetate, following a technique described elsewhere.[50] The purity of the isolated NTZ was confirmed by ^{1}H-NMR spectroscopy, employing deuterated dimethyl sulfoxide (DMSO-d_6) as solvent (500-MHz Bruker® Avance II High Resolution spectrometer, Bruker BioSpin GmbH, Rheinstetten, Germany) (Fig. 1) and melting point analysis (Fisher-Johns Melting Point Apparatus, Thermo Fisher Scientific, Inc., Waltham, MA, USA). All the solvents were of analytical or spectroscopic quality and they were used without further purification.

2.2. Synthesis of Lactosylated Derivatives

The different lactosylated derivatives were synthesized by the conventional Steglich esterification reaction as described elsewhere.[49] Briefly, the corresponding PEO–PPO copolymer (2.5–5.0 g), LA, DCC and DMAP were dissolved separately in pure DMSO (10 mL) previously dried with molecular sieves 3A (Sigma-Aldrich) for at least 24 h. LA, DCC and DMAP solutions were added successively to the copolymer solution under magnetic stirring.[49] The reaction proceeded at room temperature for 72 h. The solution was diluted in water (1:2) and dialyzed against water for four days with periodic exchanges of the dialysis medium. Finally, solutions were filtered and freeze-dried (Lyophilizer L05, F.i.c, Scientific Instrumental Manufacturing, Buenos Aires, Argentina). The number of LA units per copolymer molecule was estimated by elemental analysis;[49] substitution extents were 50% for F127
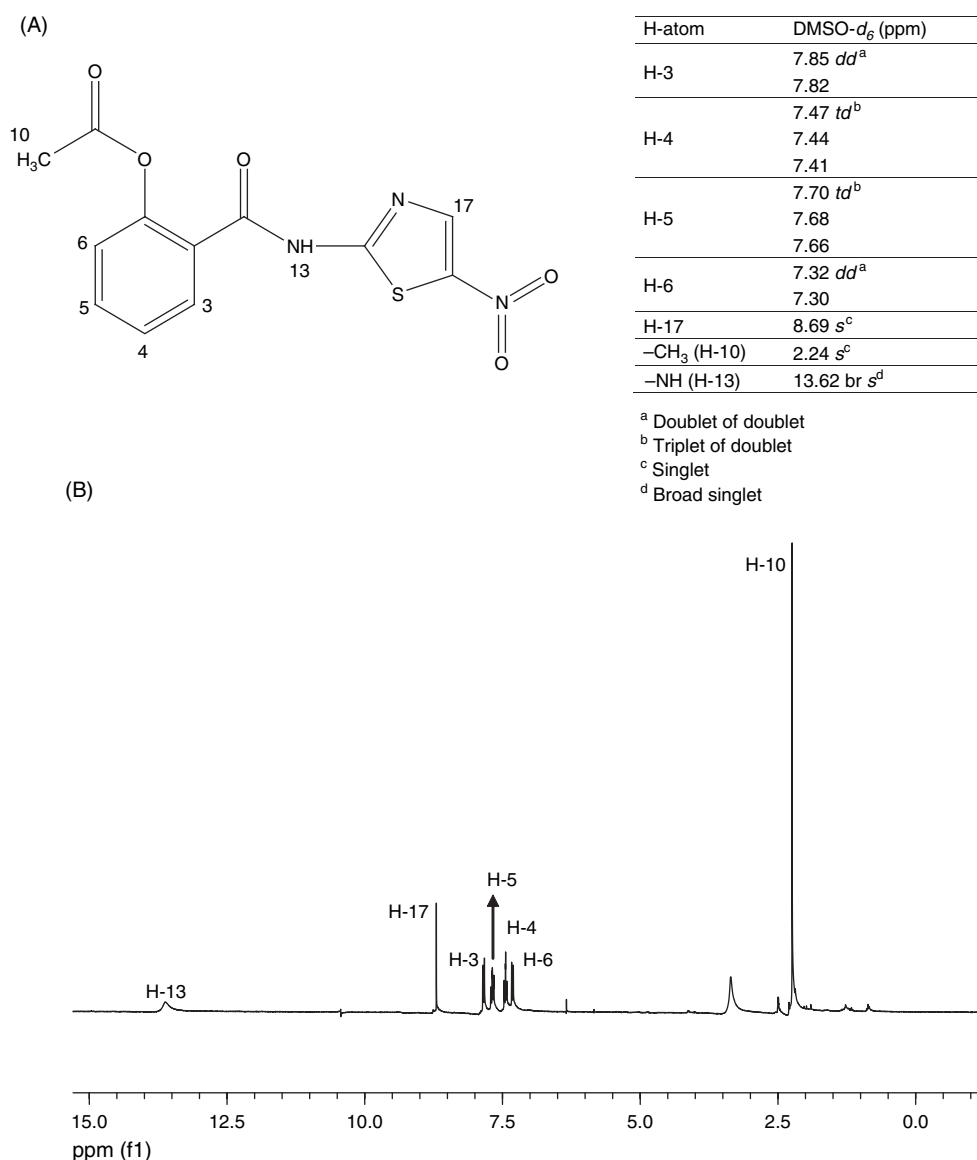
(A)

H-atom	DMSO-d_6 (ppm)
H-3	7.85 *dd*[a]
	7.82
H-4	7.47 *td*[b]
	7.44
	7.41
H-5	7.70 *td*[b]
	7.68
	7.66
H-6	7.32 *dd*[a]
	7.30
H-17	8.69 *s*[c]
−CH$_3$ (H-10)	2.24 *s*[c]
−NH (H-13)	13.62 br *s*[d]

[a] Doublet of doublet
[b] Triplet of doublet
[c] Singlet
[d] Broad singlet

(B)

Fig. 1. (A) Chemical structure of nitazoxanide (NTZ) isolated from tablets with the assignment of the corresponding ^{1}H-NMR signals and (B) ^{1}H-NMR spectrum of NTZ.

(one LA group/copolymer molecule), 25% for T1107 (one LA group/copolymer molecule) and 75% for T904 (three LA groups/copolymer molecule). The conjugates of F127, T1107 and T904 with LA are named F127-LA, T1107-LA and T904-LA.[49]

2.3. Preparation of NTZ-Loaded PMs

To produce PMs of concentrations between 1% and 10% w/v, the required amount of copolymer was solubilized in water at 4 °C and then the solution was equilibrated at 25 °C at least 24 h before use. To screen the encapsulation capacity of each type of PM, NTZ (in excess, ∼10 mg/mL copolymer solution) was added to F127, T1107 and T904 PMs (5 mL) in caramel glass vials and sealed with paraffin film. Specimens were vigorously

stirred (48 h) at room temperature to enable the incorporation of NTZ to the micelle and the resulting yellow suspensions were filtered through clarifying filters (0.45 μm, nylon membrane, Osmonics Inc., Minnesonta, MN, USA) to remove insoluble drug. The drug payload in the different systems was quantified by UV spectrophotometry ($\lambda = 282$ nm, CARY [1E] UV-Visible Spectrophotometer, Varian, Inc., Lake Forest, CA, USA) at room temperature, after the appropriate dilution. A calibration curve of NTZ in dimethylformamide (DMF) covering the range between 2.0 and 12.5 μg/mL ($R^2 > 0.999$) was used. NTZ concentrations are expressed in μg/mL or mg/mL. Copolymer solutions in DMF were used as blank. Solubility factors were calculated according to Eq. (1)

$$f_s = S_{PM}/S_{water} \tag{1}$$

Where S_{PM} and S_{water} are the apparent solubility of NTZ in the corresponding micelles and the experimental intrinsic solubility in MilliQ water (Simplicity® Water Purification System, Millipore, Billerica, MA, USA; pH = 5.8) as determined in our laboratory (6.78 μg/mL), respectively. The encapsulation capacity of 7% F127-LA, 10% T1107-LA and 5% w/v T904-LA micelles was also assessed.

Two types of mixed PMs with hydrophilic:hydrophobic copolymer weight ratios of 75:25, 50:50 and 25:75 were produced: (i) F127:T904 and T1107:T904 and (ii) F127-LA:T904 and T1107-LA:T904. The former are unmodified, while the latter are lactosylated. For this, the required amount of each copolymer was dissolved in the same aliquot of water at 4 °C and the micellar dispersion was equilibrated at 25 °C at least 24 h before use.[38, 51] The quantification of NTZ was carried out as described above.

2.4. Size and Size Distribution Analysis

The hydrodynamic diameter (D_h) and the size distribution (polydispersity index, PDI) of NTZ-free and NTZ-loaded PMs were assayed by Dynamic Light Scattering (DLS, Zetasizer Nano-ZS, Malvern Instruments, Worcestershire, UK) at a scattering angle of 173°. The Nano-ZS contains a 4 mW He–Ne laser operating at a wavelength of 633 nm, a digital correlator ZEN3600 and a Non-Invasive Back Scatter (NIBS®) technology. All the samples were analyzed at 25 and 37 °C. Refractive indices (RI) ranged between 1.333 and 1.345 and viscosities between 0.8868 and 0.8898 cP (25 °C) and 0.6852 and 0.6870 cP (37 °C). Results are expressed as mean ± S.D. of three independent samples prepared under identical conditions. Data for each single specimen was the result of at least six runs.

2.5. Physical Stability of NTZ-Loaded PMs

To evaluate the physical stability of the NTZ-loaded micelles, samples were stored at 25 and 37 °C and the drug concentration in solution was monitored over 28 days by UV spectrophotometry (see above). All the assays were conducted in triplicate and results are expressed as the mean concentration of NTZ remaining in solution ± S.D. Concomitantly, the D_h and PDI were also followed up by DLS (see above).

2.6. Data Analysis

The statistical analysis was performed by a one-way ANOVA (5% significance level, P values greater than 0.05 were considered statistically significant) combined with the Dunnett's Multiple Comparison Test or t-test (5% significance level, P values greater than 0.05 were considered statistically significant). The software used was GraphPad Prism version 5.00 for Windows (GraphPad Software Inc., USA).

3. RESULTS AND DISCUSSION

3.1. NTZ Encapsulation

NTZ is a nitrothiazole derivative with activity against various bacterial, viral, protozoal and helminthic infections (Fig. 1). Recent data have shown that NTZ is also a potent inhibitor of hepatitis B and C viruses.[18] Regardless of the relatively low lipophilicity with a log P of approximately 2.1, it displays a high melting point of 202 °C that reveals strong solute–solute interactions. These properties lead to a poor water solubility (6.78 μg/mL). Currently, the compound is formulated in suspensions and tablets.[12]

Aiming to explore the potential active targeting of NTZ to cells of the liver parenchyma by the recognition of LLRs, the present work preliminarily assessed the solubilization of NTZ within pristine and lactosylated PEO–PPO PMs. To investigate the effect of the different molecular features, the encapsulation of NTZ was initially assessed in a single PMs of three copolymers displaying different molecular weight, HLB and architecture. The presence of PMs was ensured by conducting the encapsulation assays with copolymer dispersions of concentrations between 1% and 10%, that were above the CMC values previously established for each derivative.[31, 33, 34, 49, 51] For example, 1% F127, T1107 and T904 PMs increased the solubility of NTZ from 6.78 μg/mL to 0.19 ($f_s = 28$), 0.21 ($f_s = 31$) and 0.32 mg/mL ($f_s = 47$), respectively (Table I). The low solubilization performance of these diluted micellar dispersions was probably associated with the relatively small number of micelles formed at copolymer concentrations slightly above the CMC. In general, regardless of the lower molecular weight and smaller core of T904 with respect to F127 and T1107 PMs, it showed the best encapsulation capacity owing to its greater hydrophobicity. The increase of the copolymer concentration and the formation of a greater number of micelles resulted in growing encapsulation extents. Thus, pristine 3%, 5%, 7% and 10% T904 PMs increased the solubility of NTZ to 1.10, 1.94, 2.59 and 4.13 mg/mL, representing f_s values of 162, 286, 382 and 609, respectively, these extents being significantly greater than those obtained with F127 and T1107 (Table I). F127 and T1107 followed a similar trend with growing encapsulation capacity at greater concentrations. The comparison between F127 and T1107, two copolymers of similar HLB and different molecular weight and architecture, revealed a less clear trend. On one hand, T1107 displays a greater molecular weight and larger core size that would increase the encapsulation capacity of the micelles. On the other, poloxamines are dually-responsive copolymers that display a pK_a value between 4.0 and 5.6 for the first tertiary amine group and 6.2 to 8.1 for the second one.[33, 52] In this context, at pH 5.8, poloxamines are mono or diprotonated and electrostatic repulsion hampers the micellization. At copolymer concentrations below 7%, both PMs showed very similar f_s values, differences being not statistically significant. This phenomenon

Table I. Apparent solubility (S_{PM}) and solubility factor (f_s) of NTZ within the different PMs. The intrinsic solubility of NTZ in water (S_{water}) was 6.78 mg/mL.

Type of polymeric micelle	Copolymer composition	Total copolymer concentration (% w/v)	S_{PM} (mg/mL) (±S.D.)	f_s
	F127		0.19 (0.04)	28
	T1107	1	0.21 (0.04)	31
	T904		0.32 (0.08)	47
	F127		0.40 (0.04)	59
	T1107	3	0.54 (0.03)	80
	T904		1.10 (0.09)	162
	F127		0.71 (0.03)	105
	T1107		0.66 (0.07)	97
Single	T904	5	1.94 (0.06)	286
	T904-LA*		0.49 (0.03)	72
	F127		1.01 (0.02)	149
	F127-LA**		0.15 (0.06)	22
	T1107	7	0.98 (0.09)	145
	T904		2.59 (0.02)	382
	F127		1.45 (0.04)	214
	T1107		1.81 (0.06)	267
	T1107-LA		0.98 (0.02)	145
	T904		4.13 (0.11)	609
	F127:T904 (75:25)		2.00 (0.10)	295
	F127:T904 (50:50)		2.26 (0.13)	333
	F127:T904 (25:75)	10	3.16 (0.02)	466
	T1107:T904 (75:25)		1.33 (0.04)	196
Mixed	T1107:T904 (50:50)		2.19 (0.17)	323
	T1107:T904 (25:75)		2.10 (0.06)	310
	T1107-LA:T904 (75:25)		1.04 (0.10)	153
	T1107-LA:T904 (50:50)		1.95 (0.08)	288
	T1107-LA:T904 (25:75)		3.27 (0.03)	482

Notes: f_s was calculated as the ration between S_{PM} and S_{water}. *The maximum solubility of T904-LA was 5%. **The maximum solubility of F127-LA was 7%.

would stem from the compensation of the better encapsulation of the larger T1107 core by the smaller micellization tendency of poloxamines under the slightly acid conditions of the medium employed. When the copolymer concentration was increased to 10%, the micellization of T1107 was more efficient and thus, the core size governed the encapsulation that resulted in a more marked difference.

Mixed PMs are produced by the co-micellization of two amphiphiles displaying different HLB and they have become an effective approach to optimize the encapsulation of poorly-water soluble drugs and to increase the physical stability of these colloidal systems over time.[38, 50] In this context, the encapsulation of NTZ within 10% PMs made of F127 or T1107 with growing T904 concentrations was evaluated. Results showed the sharp solubility increase of the encapsulation with respect to single F127 and T1107 PMs owing to the incorporation of the more hydrophobic T904 into the core. For example, 10% F127:T904 (75:25), F127:T904 (50:50) and F127:T904 (25:75) encapsulated 2.00 ($f_s = 295$), 2.26 ($f_s = 333$) and 3.16 mg/mL ($f_s = 466$) of NTZ (Table I). T1107:T904 PMs showed a

similar behavior, though the improvement was more moderated.

To enable the recognition of the nanocarrier by receptors that are profusely expressed in the hepatocyte (e.g., LLRs), PEO–PPOs were conjugated to lactobionic acid employing the Steglich condensation reaction. F127-LA and T1107-LA contained one LA residue per molecule, representing conjugation extents of 50% and 25%, respectively. Conversely, T904-LA contained three LA groups (75% conjugation).[49] Regardless of the lower CMC shown by lactosylated PEO–PPOs, this modification had a strong detrimental effect on the solubilization of NTZ, S_{PM} values decreasing pronouncedly from 1.94 to 0.49 mg/mL ($f_s = 72$) for 5% T904-LA, 1.01 to 0.15 mg/mL ($f_s = 22$) for 7% F127-LA and 1.81 to 0.98 mg/mL ($f_s = 145$) for 10% T1107-LA (Table I). This behavior could be probably related to a detrimental effect of NTZ on the micellization tendency of the modified amphiphile. This was supported by the large size of the NTZ-loaded micelles measured by DLS (see below). Since the lactosylation of the surface is critical to enable the active targeting, we also explored the performance of mixed 10% PMs that combined lactosylated T1107 and pristine T904. This approach relied on previous investigations showing that F127:T904 and T1107:T904 mixed micelles are most likely formed by the inclusion of the hydrophobic copolymer within the core of a micellar template formed by the hydrophilic counterpart.[38, 51] In this context, this mixed PMs are expected to display the lactose residues on the micellar surface. Results indicated that while this method was not beneficial in the case of 10% T1107-LA:T904 (75:25) due to the insufficient concentration of T904 in the micelle, the encapsulation capacity was recovered almost completely in 10% T1107-LA:T904 (25:75) PMs that showed a S_{PM} value of 3.27 mg/mL ($f_s = 482$). It is important to mention that mixed F127-LA:T904 PMs were not evaluated because of the more limited solubility of F127-LA that was 7% w/v (Table I).

3.2. Effect of NTZ Encapsulation on the Size of the Aggregates

The size is a critical parameter that governs the physical stability of the dispersions and the interaction of the drug-loaded nanocarriers with cells and tissues and it can also condition the absorption process in mucosa.[53, 54] In this context, the size and size distribution of the different unmodified and lactosylated single and mixed NTZ-loaded PMs were characterized by DLS at 25 and 37 °C; PEO–PPOs are thermo-responsive amphiphiles. Drug encapsulation leads to two possible phenomena: (i) enlargement of the micelles or (ii) secondary aggregation. The former is evidenced by a moderate size growth, while the latter generates significantly larger structures.[34–36, 55] At 25 °C, all the pristine PMs initially showed two size populations (Table II). During the first 14 days, the small size fraction

Table II. Size (Dh) and size distribution (PDI) of NTZ-loaded pristine PEO–PPO PMs at 25 and 37 °C over 28 days, as measured by DLS.

Copolymer	Concentration (% w/v)	T (°C)	Day	Peak 1[a] D_h (nm) (±S.D.)	%Intensity (± S.D.)	Peak 2[b] D_h (nm) (± S.D.)	% Intensity (± S.D.)	PDI (±S.D.)
F127	1	25	0	24.7 (1.5)	6.5 (1.3)	316.7 (17.8)	93.5 (1.3)	0.47 (0.09)
			1	26.4 (1.9)	13.9 (0.8)	307.4 (3.1)	86.1 (0.8)	0.62 (0.13)
			14	29.5 (4.6)	42.4 (11.0)	295.6 (96.9)	57.6 (11.0)	0.38 (0.05)
			28	27.4 (3.6)	46.0 (10.3)	243.6 (43.0)	54.0 (10.3)	0.33 (0.07)
		37	0	21.4 (1.1)	15.2 (1.2)	234.4 (16.8)	84.8 (1.2)	0.43 (0.14)
			1	20.1 (1.1)	8.6 (1.0)	294.6 (19.6)	91.5 (1.0)	0.37 (0.14)
			14	27.1 (0.7)	90.8 (2.9)	414.2 (100.0)	9.3 (2.9)	0.28 (0.04)
			28	27.7 (1.1)	83.6 (8.5)	1145.7 (16.0)	16.4 (8.5)	0.31 (0.07)
	3	25	0	29.3 (3.7)	6.4 (3.6)	469.0 (15.3)	93.6 (3.6)	0.44 (0.09)
			1	34.7 (4.9)	17.6 (2.2)	448.0 (18.6)	82.4 (2.2)	0.81 (0.11)
			14	26.3 (8.9)	31.6 (13.1)	200.1 (36.7)	68.4 (13.1)	0.69 (0.19)
			28	29.7 (4.4)	35.8 (10.6)	353.7 (147.5)	64.2 (10.6)	0.40 (0.10)
		37	0	20.7 (1.0)	20.1 (3.3)	337.6 (13.6)	79.9 (3.3)	0.49 (0.08)
			1	15.0 (1.0)	98.7 (0.4)	638.4 (34.3)	1.3 (0.4)	0.36 (0.01)
			14	22.8 (0.9)	91.2 (3.0)	326.5 (166.3)	8.9 (3.0)	0.25 (0.07)
			28	24.7 (0.2)	91.2 (2.3)	1481.2 (7.9)	8.8 (2.3)	0.24 (0.04)
	5	25	0	31.9 (1.9)	16.7 (2.0)	614.8 (67.4)	83.3 (2.0)	0.93 (0.09)
			1	28.8 (2.7)	25.6 (1.4)	495.7 (88.8)	74.4 (1.4)	0.61 (0.08)
			14	37.1 (9.6)	32.6 (7.0)	373.5 (134.9)	67.4 (7.0)	0.38 (0.10)
			28	37.1 (5.0)	21.6 (1.1)	941.8 (100.0)	78.4 (1.1)	0.46 (0.08)
		37	0	10.2 (0.5)	6.0 (1.8)	706.9 (64.0)	94.0 (1.8)	0.41 (0.14)
			1	13.2 (0.4)	6.5 (3.9)	610.4 (56.9)	93.5 (3.9)	0.53 (0.05)
			14	20.8 (1.2)	40.2 (0.9)	515.1 (23.1)	59.8 (0.9)	0.98 (0.01)
			28	22.7 (0.9)	84.7 (0.5)	526.1 (74.5)	15.3 (0.5)	0.35 (0.05)
	7	25	0	26.0 (6.9)	6.2 (2.7)	1072.2 (88.2)	93.8 (2.7)	0.50 (0.01)
			1	37.5 (3.5)	46.9 (3.3)	717.7 (104.0)	53.1 (3.3)	0.61 (0.09)
			14	31.7 (4.7)	49.2 (4.8)	821.6 (222.1)	50.8 (4.8)	0.54 (0.09)
			28	35.4 (1.1)	34.4 (3.1)	268.7 (44.4)	65.6 (3.1)	0.40 (0.07)
		37	0	12.5 (0.5)	3.7 (2.9)	1192.4 (89.7)	96.3 (2.9)	0.43 (0.25)
			1	16.4 (1.8)	9.4 (2.2)	951.5 (27.2)	90.6 (2.2)	0.63 (0.04)
			14	19.4 (0.6)	32.9 (1.7)	864.0 (55.6)	67.1 (1.7)	0.99 (0.02)
			28	20.9 (1.1)	70.8 (2.9)	565.2 (112.5)	29.2 (2.9)	0.50 (0.03)
	10	25	0	12.0 (0.4)	16.7 (8.0)	1882.8 (402.7)	83.3 (8.0)	0.58 (0.10)
			1	17.1 (7.1)	27.4 (4.3)	1294.0 (89.9)	72.6 (4.3)	0.92 (0.11)
			14	11.2 (1.0)	10.7 (5.1)	424.0 (19.8)	89.3 (5.1)	0.99 (0.01)
			28	19.7 (4.2)	28.7 (5.2)	804.4 (297.9)	71.3 (5.2)	0.89 (0.08)
		37	0	12.0 (0.4)	0.8 (0.7)	1873.4 (124.7)	99.2 (0.7)	0.25 (0.08)
			1	17.1 (4.6)	11.6 (3.4)	1454.2 (84.9)	88.4 (3.4)	0.64 (0.23)
			14	20.2 (1.1)	28.1 (7.1)	1650.5 (304.2)	71.9 (7.1)	0.96 (0.07)
			28	19.3 (1.6)	47.0 (6.8)	1075.0 (42.9)	53.0 (6.8)	0.67 (0.05)
T1107	1	25	0	7.8 (0.1)	2.0 (0.7)	275.4 (31.9)	98.0 (0.7)	0.32 (0.03)
			1	7.0 (0.2)	15.3 (4.2)	274.6 (22.1)	84.7 (4.2)	0.68 (0.12)
			14	6.9 (0.2)	10.8 (0.7)	243.2 (56.8)	89.2 (0.7)	0.72 (0.23)
			28	5.9 (0.8)	14.9 (0.2)	243.4 (10.7)	85.1 (0.2)	0.37 (0.02)
		37	0	14.6 (0.5)	7.5 (1.2)	242.1 (10.8)	92.5 (1.2)	0.40 (0.06)
			1	9.0 (0.5)	0.5 (0.4)	289.2 (7.1)	99.5 (0.4)	0.18 (0.01)
			14	16.9 (1.6)	4.6 (1.3)	275.8 (7.7)	95.4 (1.3)	0.29 (0.02)
			28	16.0 (0.7)	42.6 (8.2)	195.4 (32.8)	57.4 (8.2)	0.25 (0.04)
	3	25	0	5.6 (0.1)	4.7 (3.2)	396.4 (16.0)	95.3 (3.2)	0.46 (0.05)
			1	4.9 (0.3)	11.8 (1.6)	263.8 (18.6)	88.2 (1.6)	0.69 (0.09)
			14	6.3 (0.6)	18.4 (0.5)	224.3 (54.9)	81.6 (0.5)	0.83 (0.13)
			28	5.5 (0.9)	25.8 (0.4)	212.2 (21.1)	74.2 (0.4)	0.75 (0.34)
		37	0	14.0 (1.0)	2.2 (1.8)	427.0 (47.9)	97.8 (1.8)	0.32 (0.09)
			1	9.2 (0.1)	1.1 (0.5)	497.5 (35.6)	98.9 (0.5)	0.26 (0.04)
			14	14.1 (0.5)	25.3 (3.2)	405.1 (15.3)	74.7 (3.2)	0.78 (0.22)
			28	15.4 (0.7)	83.6 (3.3)	164.4 (39.4)	16.4 (3.3)	0.17 (0.06)

Table II. Continued.

Copolymer	Concentration (% w/v)	T (°C)	Day	Peak 1[a] D_h (nm) (±S.D.)	Peak 1[a] %Intensity (± S.D.)	Peak 2[b] D_h (nm) (± S.D.)	Peak 2[b] % Intensity (± S.D.)	PDI (±S.D.)
	5	25	0	5.6 (0.4)	2.8 (1.7)	497.4 (46.2)	97.3 (1.7)	0.59 (0.05)
			1	6.7 (0.5)	19.9 (2.1)	274.0 (88.8)	80.1 (2.1)	0.87 (0.16)
			14	6.1 (0.2)	19.1 (1.0)	397.2 (31.9)	80.9 (1.0)	0.61 (0.20)
			28	6.0 (0.3)	28.2 (3.0)	263.5 (23.2)	71.8 (3.0)	0.80 (0.27)
		37	0	15.7 (1.9)	7.6 (4.3)	435.2 (19.3)	92.4 (4.3)	0.53 (0.06)
			1	13.2 (0.7)	4.2 (2.5)	519.0 (25.1)	95.8 (2.5)	0.36 (0.06)
			14	12.1 (0.6)	15.8 (2.6)	645.1 (53.2)	84.2 (2.6)	0.89 (0.15)
			28	14.5 (1.2)	78.6 (2.0)	230.0 (106.8)	21.4 (2.0)	0.31 (0.05)
	7	25	0	5.2 (0.3)	5.4 (3.6)	626.3 (113.5)	94.6 (3.6)	0.53 (0.05)
			1	5.6 (0.4)	4.1 (2.8)	497.9 (104.0)	95.9 (2.8)	0.94 (0.07)
			14	5.9 (1.8)	16.2 (1.7)	575.8 (95.7)	83.8 (1.7)	0.61 (0.09)
			28	5.7 (0.7)	29.1 (1.2)	396.2 (53.8)	70.9 (1.2)	0.80 (0.28)
		37	0	15.0 (0.2)	3.0 (1.8)	740.8 (80.5)	97.0 (1.8)	0.31 (0.08)
			1	9.7 (0.4)	7.2 (1.1)	645.1 (60.4)	92.8 (1.1)	0.33 (0.08)
			14	10.9 (0.6)	14.3 (2.7)	823.4 (97.6)	85.7 (2.7)	0.82 (0.22)
			28	14.9 (1.9)	74.0 (2.3)	424.5 (157.6)	26.0 (2.3)	0.42 (0.09)
	10	25	0	5.3 (0.6)	11.7 (3.4)	1255.5 (73.4)	88.3 (3.4)	0.67 (0.17)
			1	20.0 (6.1)	14.9 (3.4)	320.2 (89.9)	85.1 (3.4)	0.99 (0.01)
			14	5.0 (0.1)	18.2 (3.2)	984.7 (100.0)	81.8 (3.2)	0.68 (0.22)
			28	11.5 (4.4)	22.2 (2.0)	530.6 (78.0)	77.8 (2.0)	0.54 (0.17)
		37	0	10.4 (3.3)	18.1 (8.9)	513.9 (22.4)	81.9 (8.9)	0.78 (0.05)
			1	9.1 (1.9)	8.8 (4.0)	1006.9 (32.2)	91.2 (4.0)	0.37 (0.09)
			14	8.4 (1.8)	11.4 (3.2)	1048.3 (303.3)	88.6 (3.2)	0.29 (0.07)
			28	18.6 (7.1)	45.4 (2.5)	853.8 (134.0)	54.6 (2.5)	0.69 (0.02)
T904	1	25	0	9.7 (0.7)	20.8 (1.7)	290.2 (26.0)	79.2 (1.7)	0.63 (0.18)
			1	13.9 (0.1)	53.1 (9.6)	234.8 (3.1)	46.9 (9.6)	0.98 (0.01)
			14	5.4 (0.2)	42.8 (3.4)	221.8 (55.0)	57.2 (3.4)	0.29 (0.04)
			28	4.7 (0.5)	32.5 (4.2)	267.8 (10.7)	67.5 (4.2)	0.66 (0.18)
		37	0	11.2 (0.7)	88.6 (2.8)	192.0 (59.5)	11.4 (2.8)	0.23 (0.08)
			1	11.1 (0.3)	93.6 (0.7)	240.4 (67.9	6.4 (0.7)	0.22 (0.11)
			14	10.7 (0.4)	88.2 (3.4)	246.4 (40.6)	11.8 (3.4)	0.24 (0.08)
			28	12.0 (0.4)	86.1 (1.6)	243.7 (89.6)	13.9 (1.6)	0.18 (0.01)
	3	25	0	10.0 (0.5)	12.8 (2.1)	498.5 (47.0)	87.2 (2.1)	0.51 (0.11)
			1	16.6 (3.0)	5.3 (0.6)	410.0 (18.6)	94.7 (0.6)	0.54 (0.03)
			14	4.6 (0.3)	9.6 (3.1)	233.8 (25.6)	90.4 (3.1)	0.50 (0.08)
			28	4.9 (0.2)	13.6 (4.0)	173.0 (21.1)	86.4 (4.0)	0.51 (0.18)
		37	0	12.6 (1.0)	73.3 (6.6)	252.7 (11.6)	26.7 (6.6)	0.43 (0.14)
			1	11.5 (1.0)	80.6 (5.5)	192.5 (25.7)	19.4 (5.5)	0.23 (0.14)
			14	10.4 (0.1)	81.7 (0.8)	206.3 (0.8)	18.3 (0.8)	0.57 (0.01)
			28	11.9 (0.6)	77.6 (6.7)	289.4 (36.8)	22.4 (6.7)	0.27 (0.09)
	5	25	0	17.5 (0.3)	2.0 (0.8)	489.2 (79.4)	98.0 (0.8)	0.42 (0.06)
			1	7.8 (0.2)	11.0 (1.3)	379.7 (88.8)	89.0 (1.3)	0.65 (0.01)
			14	4.5 (0.1)	29.7 (3.3)	271.4 (17.9)	70.3 (3.3)	0.96 (0.08)
			28	25.7 (3.8)	17.8 (2.6)	251.1 (23.2)	82.2 (2.6)	0.71 (0.04)
		37	0	10.1 (0.3)	35.7 (3.0)	265.3 (27.2)	64.3 (3.0)	0.24 (0.08)
			1	11.4 (0.9)	41.4 (10.0)	281.7 (74.4)	58.6 (10.0)	0.57 (0.31)
			14	11.4 (0.4)	59.3 (4.8)	507.8 (61.4)	40.7 (4.8)	0.46 (0.08)
			28	10.8 (0.6)	68.3 (0.8)	409.9 (55.2)	31.7 (0.8)	0.37 (0.10)
	7	25	0	11.7 (4.7)	11.6 (2.1)	363.2 (60.3)	88.4 (2.1)	0.55 (0.05)
			1	6.5 (2.4)	14.6 (1.1)	229.8 (104.0)	85.4 (1.1)	0.98 (0.01)
			14	23.1 (2.8)	26.3 (3.4)	336.5 (66.0)	73.7 (3.4)	0.86 (0.28)
			28	27.4 (1.9)	31.3 (3.5)	277.9 (53.8)	68.7 (3.5)	0.80 (0.30)
		37	0	9.6 (0.4)	41.2 (5.3)	279.2 (74.3)	58.8 (5.3)	0.49 (0.13)
			1	11.0 (0.9)	53.2 (3.6)	384.8 (35.8)	46.8 (3.6)	0.50 (0.01)
			14	10.7 (0.2)	66.4 (2.2)	494.8 (59.0)	33.6 (2.2)	0.40 (0.02)
			28	10.4 (0.7)	84.8 (0.8)	204.3 (8.3)	15.2 (0.8)	0.27 (0.07)

RESEARCH ARTICLE

Table II.   Continued.

Copolymer	Concentration (% w/v)	T (°C)	Day	Peak 1[a] D_h (nm) (±S.D.)	%Intensity (± S.D.)	Peak 2[b] D_h (nm) (± S.D.)	% Intensity (± S.D.)	PDI (±S.D.)
	10	25	0	18.8 (0.2)	1.0 (0.7)	674.2 (98.3)	99.0 (0.7)	0.60 (0.09)
			1	8.9 (2.1)	14.9 (0.9)	396.9 (89.9)	85.1 (0.9)	0.76 (0.01)
			14	16.5 (1.8)	22.0 (2.6)	417.3 (38.4)	78.0 (2.6)	0.98 (0.01)
			28	16.9 (4.3)	25.1 (3.5)	426.3 (78.0)	74.9 (3.5)	0.98 (0.02)
		37	0	8.9 (1.1)	48.0 (7.3)	433.2 (108.4)	52.0 (7.3)	0.67 (0.07)
			1	11.9 (1.8)	67.6 (3.5)	397.8 (38.6)	32.4 (3.5)	0.32 (0.06)
			14	12.3 (1.9)	70.9 (7.4)	453.2 (75.1)	29.1 (7.4)	0.28 (0.03)
			28	11.8 (0.9)	88.2 (0.6)	354.1 (83.8)	11.8 (0.6)	0.26 (0.05)

Notes: [a]Size population of smaller size; [b]Size population of larger size.

was usually the less intense one; sizes between 5 and 38 nm corresponded to unimers, incomplete aggregates and drug-loaded PMs slightly expanded with respect to drug-free micelles due to the incorporation of the drug into the core. Noteworthy, the % intensity of small size fraction moderately increased at 28 days, being this increase more noticeable at 37 °C (up to 91%) than at 25 °C (up to 46%). This phenomenon probably stemmed from the gradual release and precipitation of NTZ and the subsequent shrinkage of the micelles due to a decrease of the drug payload. Conversely, the presence of large structures (160–1900 nm) revealed that micellar fusion was also a

mechanism taking place (Table II). The bimodal aggregation pattern was supported by relatively high PDI values >0.17. The size pattern remained almost unchanged over 4 weeks. At 37 °C, the bimodal aggregation pattern was conserved. In addition, PMs usually showed a mild to substantial shrinkage owing to the thermo-responsive nature of PEO–PPOs. For example, the size of the minor and the major intensity fractions of 1% and 3% pure F127 micelles decreased from 25 and 317 nm and 29 and 469 nm at 25 °C to 21 and 234 nm and 21 and 338 nm, respectively, at 37 °C. More concentrated micelles showed more moderate changes. T1107 micelles followed a similar trend.

Table III.   Size (D_h) and size distribution (PDI) of NTZ-loaded lactosylated PEO–PPO PMs at 25 and 37 °C over 28 days, as measured by DLS.

Copolymer	Concentration (% w/v)	T (°C)	Day	Peak 1[a] D_h (nm) (±S.D.)	%Intensity (± S.D.)	Peak 2[b] D_h (nm) (± S.D.)	% Intensity (± S.D.)	PDI (±S.D.)
T904-LA	5	25	0	12.9 (1.3)	33.6 (2.6)	283.9 (34.8)	66.4 (2.6)	0.38 (0.08)
			1	9.6 (0.5)	29.0 (3.1)	214.8 (26.1)	71.0 (3.1)	0.52 (0.16)
			14	9.2 (2.8)	20.4 (10.4)	289.1 (49.8)	79.6 (10.4)	0.47 (0.08)
			28	10.0 (0.8)	29.2 (11.7)	401.1 (49.6)	70.8 (11.7)	0.82 (0.10)
		37	0	11.1 (1.3)	63.0 (6.1)	214.8 (54.1)	37.0 (6.1)	0.43 (0.16)
			1	13.5 (0.9)	62.4 (7.0)	233.6 (74.8)	37.6 (7.0)	0.32 (0.04)
			14	12.9 (1.1)	70.0 (15.2)	233.9 (42.4)	30.0 (15.2)	0.26 (0.08)
			28	12.1 (0.9)	46.9 (2.3)	712.4 (221.4)	53.1 (2.3)	0.48 (0.08)
F127-LA	7	25	0	28.4 (5.6)	67.4 (2.9)	320.4 (108.7)	32.6 (2.9)	0.44 (0.09)
			1	39.6 (1.6)	75.1 (3.5)	864.2 (205.3)	24.9 (3.5)	0.63 (0.05)
			14	5.2 (0.3)	17.7 (0.6)	49.4 (1.0)	82.3 (0.6)	0.47 (0.11)
			28	5.0 (0.2)	17.4 (1.4)	41.3 (1.0)	82.6 (1.4)	0.22 (0.05)
		37	0	16.6 (1.6)	66.6 (1.6)	367.9 (107.9)	33.4 (1.6)	0.75 (0.15)
			1	19.8 (1.0)	79.9 (2.5)	426.1 (125.4)	20.1 (2.5)	0.25 (0.04)
			14	23.7 (0.4)	74.9 (3.1)	834.3 (70.5)	25.1 (3.1)	0.47 (0.14)
			28	26.5 (2.3)	85.3 (4.9)	442.3 (75.2)	14.7 (4.9)	0.34 (0.08)
T1107-LA	10	25	0	5.0 (0.2)	34.1 (1.2)	871.0 (85.6)	65.9 (1.2)	0.81 (0.13)
			1	11.3 (1.1)	27.2 (0.9)	563.6 (41.8)	72.8 (0.9)	0.81 (0.18)
			14	25.2 (1.9)	4.5 (2.2)	496.1 (39.1)	95.5 (2.2)	0.51 (0.04)
			28	27.1 (2.5)	3.6 (1.8)	448.5 (57.6)	96.4 (1.8)	0.51 (0.04)
		37	0	11.5 (1.2)	53.4 (4.0)	1033.4 (315.9)	46.6 (4.0)	0.55 (0.05)
			1	15.6 (1.1)	48.2 (6.3)	607.8 (192.7)	51.8 (6.3)	0.63 (0.09)
			14	8.9 (1.5)	40.5 (2.8)	628.0 (266.8)	59.5 (2.8)	0.87 (0.09)
			28	25.4 (2.9)	35.8 (5.1)	452.7 (88.2)	64.2 (5.1)	0.47 (0.08)

Notes: [a]Size population of smaller size; [b]Size population of larger size.

Table IV. Size (D_h) and size distribution (PDI) of NTZ-loaded mixed PEO–PPO PMs at 25 and 37 °C over 28 days, as measured by DLS.

Copolymer	Copolymer composition	T (°C)	Day	Peak 1[a] D_h (nm) ($\pm$S.D.)	%Intensity ($\pm$ S.D.)	Peak 2[b] D_h (nm) ($\pm$ S.D.)	% Intensity ($\pm$ S.D.)	PDI ($\pm$S.D.)
F127:T904	75:25	25	0	28.7 (1.3)	43.2 (0.7)	1291.3 (49.0)	56.8 (0.7)	0.68 (0.04)
			1	29.4 (2.4)	45.5 (2.6)	1278.3 (300.2)	54.5 (2.6)	0.61 (0.09)
			14	22.2 (2.3)	27.3 (2.7)	626.2 (91.9)	72.7 (2.7)	0.52 (0.16)
			28	42.4 (2.1)	40.6 (7.6)	694.3 (33.9)	59.4 (7.6)	0.58 (0.15)
	50:50		0	25.0 (2.2)	49.8 (3.5)	727.7 (16.3)	50.2 (3.5)	0.51 (0.20)
			1	21.5 (2.5)	51.4 (3.2)	785.0 (132.9)	48.6 (3.2)	0.57 (0.18)
			14	24.8 (2.0)	66.3 (4.8)	653.0 (94.5)	33.7 (4.8)	0.97 (0.06)
			28	23.0 (2.6)	36.1 (6.1)	654.6 (55.1)	63.9 (6.1)	0.73 (0.08)
	25:75		0	12.5 (2.4)	23.6 (1.9)	586.9 (118.0)	76.4 (1.9)	0.72 (0.17)
			1	10.9 (3.0)	36.8 (5.9)	246.9 (50.0)	63.2 (5.9)	0.96 (0.03)
			14	12.7 (2.1)	27.2 (4.5)	411.9 (48.5)	72.8 (4.5)	0.87 (0.07)
			28	19.4 (5.0)	47.9 (2.0)	270.6 (20.0)	52.1 (2.0)	0.59 (0.12)
	75:25	37	0	19.4 (3.0)	39.8 (9.4)	152.0 (52.0)	60.2 (9.4)	0.78 (0.10)
			1	18.1 (2.8)	62.6 (5.5)	1204.7 (408.6)	37.4 (5.5)	0.43 (0.11)
			14	15.1 (1.1)	58.9 (5.2)	531.2 (141.4)	41.1 (5.2)	0.61 (0.15)
			28	17.0 (1.4)	50.7 (4.5)	950.5 (31.8)	49.3 (4.5)	0.44 (0.06)
	50:50		0	14.3 (1.0)	39.5 (3.2)	448.7 (181.9)	60.5 (3.2)	0.41 (0.11)
			1	14.3 (0.6)	70.4 (1.6)	810.2 (147.7)	29.6 (1.6)	0.47 (0.01)
			14	13.1 (0.6)	64.6 (1.6)	1009.0 (188.2)	35.4 (1.6)	0.54 (0.05)
			28	13.7 (0.4)	50.7 (1.7)	668.0 (118.5)	49.3 (1.7)	0.69 (0.27)
	25:75		0	11.0 (1.2)	39.7 (4.2)	173.8 (57.0)	60.3 (4.2)	0.24 (0.01)
			1	10.3 (0.7)	26.8 (1.2)	717.7 (45.6)	73.2 (1.2)	0.99 (0.01)
			14	11.1 (0.9)	38.1 (1.6)	844.6 (63.8)	61.9 (1.6)	0.87 (0.05)
			28	10.7 (0.6)	43.9 (1.5)	635.5 (104.8)	56.1 (1.5)	0.48 (0.17)
T1107:T904	75:25	25	0	21.1 (2.3)	46.3 (2.9)	477.1 (99.3)	53.7 (2.9)	0.43 (0.08)
			1	26.8 (0.3)	49.5 (2.3)	857.5 (40.5)	50.5 (2.3)	0.81 (0.04)
			14	14.5 (0.9)	15.5 (3.7)	500.8 (133.9)	84.5 (3.7)	0.58 (0.09)
			28	20.7 (1.5)	44.8 (9.1)	453.4 (100.0)	55.2 (9.1)	0.81 (0.03)
	50:50		0	21.5 (1.1)	39.1 (2.5)	714.3 (68.3)	60.9 (2.5)	0.98 (0.03)
			1	21.1 (1.1)	36.5 (2.1)	618.3 (189.2)	63.5 (2.1)	0.62 (0.29)
			14	14.9 (1.5)	38.5 (3.8)	466.2 (96.6)	61.5 (3.8)	0.51 (0.17)
			28	15.7 (2.5)	46.9 (3.9)	451.1 (86.9)	53.1 (3.9)	0.63 (0.12)
	25:75		0	14.5 (1.8)	28.3 (2.1)	616.0 (124.2)	71.7 (2.1)	0.69 (0.20)
			1	10.7 (0.3)	21.5 (4.7)	434.8 (99.6)	78.5 (4.7)	0.99 (0.02)
			14	21.1 (0.7)	24.8 (3.7)	680.2 (96.6)	75.2 (3.7)	0.60 (0.07)
			28	15.2 (0.5)	44.8 (6.9)	335.8 (71.6)	55.2 (6.9)	0.52 (0.15)
	75:25	37	0	22.8 (5.9)	45.5 (3.4)	704.4 (162.0)	54.5 (3.4)	0.45 (0.12)
			1	21.7 (0.3)	31.8 (5.1)	860.7 (116.2)	63.2 (5.1)	0.64 (0.10)
			14	10.0 (1.7)	36.2 (2.3)	424.4 (84.2)	63.8 (2.3)	0.46 (0.06)
			28	10.0 (0.8)	43.8 (8.8)	287.8 (44.8)	56.2 (8.8)	0.86 (0.08)
	50:50		0	14.5 (1.9)	36.8 (6.0)	445.4 (194.7)	63.2 (6.0)	0.38 (0.10)
			1	16.8 (4.2)	51.9 (2.6)	297.1 (55.9)	48.1 (2.6)	0.52 (0.14)
			14	10.2 (0.5)	60.1 (4.6)	378.8 (73.7)	39.9 (4.6)	0.29 (0.04)
			28	13.1 (3.9)	43.8 (7.6)	622.9 (101.5)	56.2 (7.6)	0.57 (0.10)
	25:75		0	9.8 (0.1)	36.2 (1.0)	590.2 (16.9)	63.8 (1.0)	0.93 (0.07)
			1	9.5 (0.1)	38.2 (1.9)	547.2 (28.2)	61.8 (1.9)	0.89 (0.03)
			14	10.7 (0.6)	44.6 (1.4)	506.4 (96.4)	55.4 (1.4)	0.70 (0.20)
			28	11.2 (0.7)	42.6 (3.1)	677.7 (74.6)	57.4 (3.1)	0.77 (0.06)
T1107-LA:T904	75:25	25	0	19.3 (6.7)	42.0 (1.3)	430.9 (90.1)	58.0 (1.3)	0.61 (0.12)
			1	20.0 (6.3)	25.3 (1.7)	540.2 (92.9)	74.7 (1.7)	0.70 (0.03)
			14	32.5 (0.5)	47.4 (3.0)	540.4 (56.0)	52.6 (3.0)	0.67 (0.13)
			28	33.2 (0.3)	48.6 (5.6)	542.6 (28.8)	51.4 (5.6)	0.95 (0.08)
	50:50		0	12.0 (0.9)	43.5 (1.3)	1888.3 (600.0)	56.5 (1.3)	0.88 (0.08)
			1	10.7 (3.7)	8.3 (2.3)	500.0 (257.4)	91.7 (2.3)	0.93 (0.12)
			14	28.3 (4.6)	69.3 (3.5)	594.3 (54.3)	30.7 (3.5)	0.88 (0.14)
			28	36.2 (6.8)	51.7 (6.2)	538.2 (50.0)	48.3 (6.2)	0.95 (0.04)
	25:75		0	18.4 (0.8)	54.7 (2.3)	462.8 (86.5)	45.3 (2.3)	0.41 (0.09)
			1	21.3 (1.1)	29.6 (0.6)	670.0 (78.6)	70.4 (0.6)	0.86 (0.08)
			14	20.7 (1.5)	45.2 (1.2)	465.4 (55.8)	54.8 (1.2)	0.53 (0.18)
			28	31.9 (7.1)	35.4 (1.5)	427.9 (97.3)	64.6 (1.5)	0.55 (0.02)

RESEARCH ARTICLE

Table IV.   Continued.

Copolymer	Copolymer composition	T (°C)	Day	Peak 1[a]		Peak 2[b]		
				D_h (nm) (±S.D.)	%Intensity (± S.D.)	D_h (nm) (± S.D.)	% Intensity (± S.D.)	PDI (±S.D.)
	75:25	37	0	13.0 (2.2)	50.6 (2.0)	308.1 (79.8)	49.4 (2.0)	0.67 (0.15)
			1	7.0 (1.3)	24.2 (1.0)	341.1 (61.3)	75.8 (1.0)	0.99 (0.01)
			14	22.2 (7.1)	52.3 (8.5)	755.1 (91.9)	47.7 (8.5)	0.68 (0.10)
			28	12.2 (1.1)	24.9 (6.4)	362.0 (26.1)	75.1 (6.4)	0.44 (0.13)
	50:50		0	13.3 (1.5)	2.7 (2.2)	238.0 (80.4)	97.3 (2.2)	0.89 (0.06)
			1	19.0 (3.2)	45.5 (3.8)	809.2 (54.2)	54.5 (3.8)	0.70 (0.06)
			14	16.6 (4.2)	68.9 (1.3)	395.1 (93.6)	31.1 (1.3)	0.36 (0.09)
			28	11.2 (0.4)	48.8 (9.1)	272.0 (99.3)	51.2 (9.1)	0.30 (0.04)
	25:75		0	11.5 (0.7)	23.0 (4.4)	243.6 (104.5)	77.0 (4.4)	0.32 (0.08)
			1	13.3 (2.4)	46.7 (3.7)	546.0 (96.8)	53.3 (3.7)	0.55 (0.08)
			14	15.0 (3.1)	74.7 (3.2)	449.8 (92.5)	25.3 (3.2)	0.37 (0.01)
			28	12.7 (2.0)	38.8 (3.3)	233.9 (70.9)	61.2 (3.3)	0.22 (0.02)

*The total copolymer concentration is 10% w/v; [a]Size population of smaller size; [b]Size population of larger size.
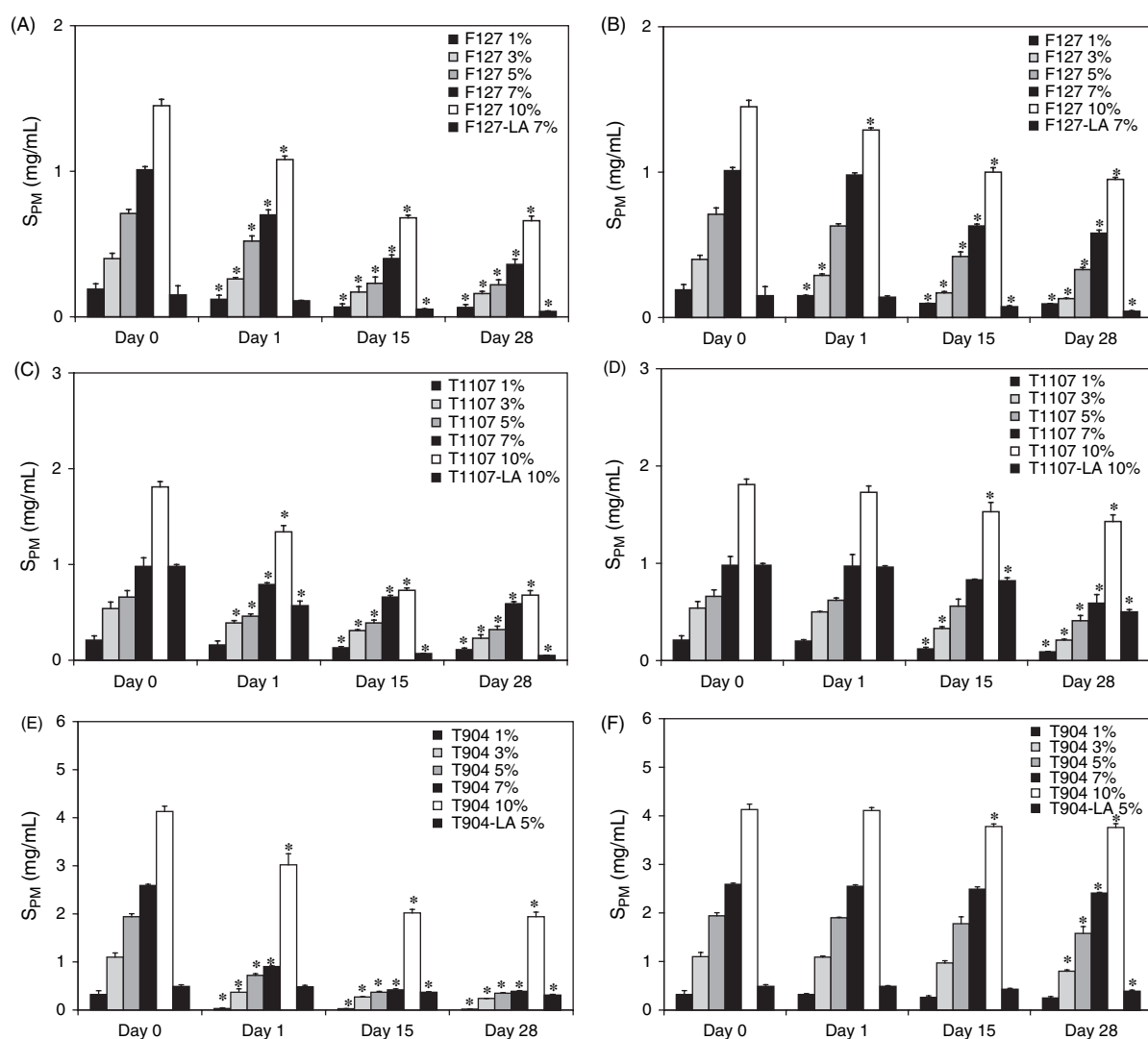
Fig. 2. Physical stability of NTZ-loaded single PMs as estimated by NTZ concentration, over 28 days. (A) F127 and F127-LA at 25 °C, (B) F127 and F127-LA at 37 °C, (C) T1107 and T1107-LA at 25 °C, (D) T1107 and T1107-LA at 37 °C, (E) T904 and T904-LA at 25 °C and (F) T904 and T904-LA at 37 °C. *Statistically significant decrease of NTZ payload when compared to the concentration day 0 ($P < 0.05$).

This behavior was more remarkable for the more hydrophobic T904. In general, PDI values remained unchanged though a slight decrease would suggest a more complete micellization (Table II). Single lactosylated and mixed PMs showed similar aggregation patterns (Tables III, IV). Generally, a higher concentration of T904 in the mixed PMs led to smaller sizes at both temperatures (Table IV). This behavior became more notorious in the F127:T904 mixed PMs (Table IV).

3.3. Physical Stability of NTZ-Loaded Micelles

Depending on the properties of the encapsulated drug and the copolymer, drug-loaded micelles can undergo a destabilization process that is characterized by the gradual crystallization and precipitation of the drug. To evaluate the

physical stability of NTZ-loaded PMs, the different samples were stored at 25 and 37 °C and the NTZ content and the micellar size and PDI monitored over 28 days by UV and DLS, respectively. At 25 °C, pristine F127 and T1107 PMs showed a gradual decreased of the solubilized NTZ to 34–46% and 38–52% of the initial concentration at day 28 (Figs. 2(A), (C)). NTZ-loaded T1107 PMs were slightly more stable than the F127 counterparts due to a greater molecular weight. T904 PMs followed a similar trend though they were much more unstable with a final concentration drop that ranged between 53% and 94% (Fig. 2(E)). This relatively poor performance could be associated with two different phenomena, the high crystallization trend of NTZ (as evidenced by its high melting point) and the incomplete micellization of PEO–PPOs at this temperature. Also, these concentration drops were more evident
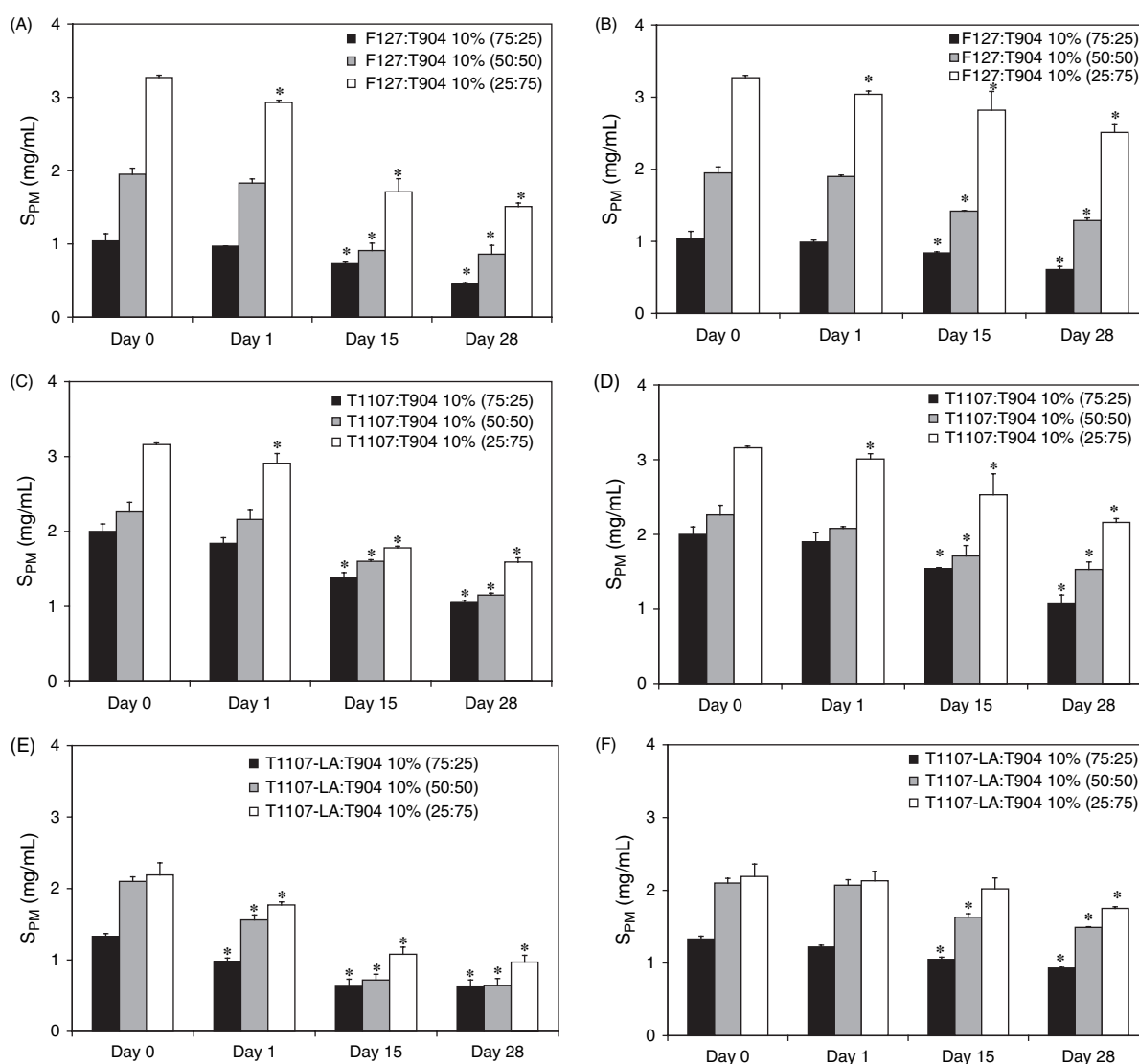

Fig. 3. Physical stability of the different NTZ-loaded mixed PMs (10% w/v of total copolymer concentration) as estimated by NTZ concentration, over 28 days. (A) F127:T904 at 25 °C, (B) F127:T904 at 37 °C, (C) T1107:T904 at 25 °C, (D) T1107:T904 at 37 °C, (E) T1107-LA:T904 at 25 °C and (F) T1107-LA:T904 at 37 °C. *Statistically significant decrease of the NTZ payload when compared to the concentration at day 0 ($P < 0.05$).

RESEARCH ARTICLE

at lower concentrations of T904 in the PMs (e.g., 1%, Fig. 2(E)). Regardless of the greater hydrophobicity, T904 displays a smaller molecular weight and a greater CMC that rendered the systems more unstable. Thus, at the lower temperature, the CMC would play a more important role in the stability of the systems. At 37 °C, all the pristine PMs showed a substantially greater physical stability with a stability order of T904 ≫ T1107 > F127 (Figs. 2(B), (D), (F)); e.g., 10% F127, T1107 and T904 PMs resulted in remaining NTZ payloads of 66%, 79% and 91%, respectively, at day 28. The greater stability of T904 PMs that at the same time display the highest NTZ encapsulation capacity probably relied on the stronger interaction of the drug with a more hydrophobic core. Also, more concentrated systems were usually more stable. At 25 °C, single 5% T904-LA, 7% F127-LA and 10% T1107-LA PMs were much less stable than their unmodified counterparts. At a higher temperature, this phenomenon was partially reverted, though final NTZ payloads remained below the extents observed for unmodified PMs. Aiming to attain PMs with greater encapsulation capacity and physical stability, mixed F127:T904 and T1107:T904 PMs were explored. These systems were more stable and, consequently, they showed a slighter drop of the NTZ concentration than pure T904 (Figs. 3(A)–(D)). In addition, the ratio between both copolymers did not play a critical role. Also here, drug-loaded PMs were more stable at 37 than 25 °C. Lactosylation had a beneficial effect on the stability of the mixed micelles (Figs. 3(E), (F)). For example, at 25 °C, the initial NTZ concentration in T1107-LA:T904 (75:25), T1107-LA:T904 (50:50) and T1107-LA:T904 (25:75) PMs decayed from 1.33, 2.10 and 2.19 to 0.62, 0.64 and 0.97 mg/mL at day 28. The NTZ concentration decrease was less pronounced at 37 °C with final concentrations remaining between 70–80% of the initial ones, at day 28.

The stability was also estimated by following up the size and size distribution of the different NTZ-loaded micelles over time. Irrespectively of the temperature, the decrease of the NTZ concentration was usually accompanied by a decrease of the micellar size due to the shrinkage of the PMs over drug precipitation (Tables II–IV). However, the analysis of this phenomenon was difficult and some systems showed the opposite, revealing that a re-aggregation process might be taking place.

4. CONCLUSIONS

In the first report investigating the nanoencapsulation of NTZ, we investigated the ability of pristine and lactosylated single and mixed PEO–PPO PMs to water-solubilize this drug. The best encapsulation performance was attained with 10% T904 (S_{PM} = 4.13 mg/mL). Conversely, lactosylation of T904 had a strong detrimental effect on the encapsulation, leading to a sharp decrease of the S_{PM} to 0.49 mg/mL. The co-micellization of highly

hydrophilic F127 and T1107 with T904 enhanced the NTZ encapsulation capacity with respect to pristine F127 and T1107 PMs. Moreover, mixed PMs produced with lactosylated F127 and T1107 as the hydrophilic component and T904 as the hydrophobic one considerably improved the water-solubility of NTZ with respect to pure F127 and T1107 and resulted in drug cargos comparable to those of pure T904. Strategies to target drug treatments to liver parenchyma represent an opportunity to enhance therapeutic outcomes in hepatic diseases where many current treatment regimes are incompletely effective and produce serious adverse effects in other non-target organs. In this context, lactosylated mixed PMs open the possibility of the active targeting of NTZ to hepatocytes for the more effective therapy of viral hepatitis that are currently being treated with NTZ in clinical trials.

References and Notes

1. L. G. Guidotti and F. V. Chisari, *Annu. Rev. Patol. Mech. Dis.* 1, 23 (**2006**).
2. T. Block, A. S. Mehta, and W. T. London, *Cancer Biomark.* 9, 375 (**2011**).
3. P. P. Michielsen, S. M. Francque, and J. L. van Dongen, *World J. Surg. Oncol.* 3, 27 (**2005**).
4. S. F. Altekruse, K. A. McGlynn, and M. E. Reichman, *J. Clin. Oncol.* 27, 1485 (**2009**).
5. Cancer. World Health Organization. (**2012**), http://www.who.int/mediacentre/factsheets/fs297/en/
6. M. L. Cuestas, V. L. Mathet, J. R. Oubiña, and A. Sosnik, *Pharm. Res.* 27, 1184 (**2010**).
7. R. J. Glisoni, D. A. Chiappetta, L. M. Finkielstein, A. G. Moglioni, and A. Sosnik, *New J. Chem.* 34, 2047 (**2010**).
8. R. J. Glisoni, D. A. Chiappetta, A. G. Moglioni and A. Sosnik, *Pharm. Res.* 29, 739 (**2012**).
9. R. J. Glisoni, M. L. Cuestas, V. Mathet, J. Oubiña, A. G. Moglioni, and A. Sosnik, *Eur. J. Pharm. Sci.* 47, 596 (**2012**).
10. V. R. Anderson and M. P. Curran, *Drugs* 67, 1947 (**2007**).
11. J. O. Juan, N. Lopez Chegne N, G. Gargala, and L. Favennec, *Transact. Royal Soc. Tropical Med. Hyg.* 96, 196 (**2002**).
12. L. M. Fox and L. D. Saravolatz, *Clin. Infect. Dis.* 40, 1173 (**2005**).
13. E. Diaz, J. Mondragon, E. Ramirez, and R. Bernal, *Am. J. Tropical Med. Hyg.* 68, 384 (**2003**).
14. L. Favennec, J. J. Ortiz, G. Gargala, N. Lopez Chegne, A. Ayoub, and J. F. Rossignol, *Aliment. Pharmacol. Ther.* 17, 265 (**2003**).
15. D. M. Musher, N. Logan, R. J. Hamill, H. L. DuPont, A. Lentnek, A. Gupta, and J.-F. Rossignol, *Clin. Infect. Dis.* 43, 421 (**2006**).
16. L. P. De Carvalho, C. M. Darby, K. Y. Rhee, and C. Natahan, *ACS Med. Chem. Lett.* 2, 849 (**2011**).
17. J. B. Watson and S. F. Moss, *Am. J. Gastroenterol.* 106, 1976 (**2011**).
18. J. F. Rossignol and Y. M. El-Gohary, *Aliment. Pharmacol. Ther.* 24, 1423 (**2006**).
19. J. F. Rossignol, M. Abu-Zekry, A. Hussein, and M. G. Santoro, *Lancet* 368, 124 (**2006**).

RESEARCH ARTICLE

20. B. E. Korba, A. B. Montero, K. Farrar, K. Gaye, S. Mukeriee, M. S. Ayers, and J. F. Rossignol, *Antiviral Res.* 77, 56 (**2008**).

21. E. B. Keffee and J. F. Rossignol, *World J. Gastroenterol.* 15, 1805 (**2009**).

22. A. V. Stachulski, C. Pidathala, E. C. Row, R. Sharma, N. G. Berry, A. S. Lawrenson, S. L. Moores, M. Iqbal, J. Bentley, S. A. Allman, G. Edwards, A. Helm, J. Hellier, B. E. Korba, J. E. Semple, and J. F. Rossignol, *J. Med. Chem.* 54, 8670 (**2011**).

23. I. Mederacke and H. Wedemeyer, *Ann. Hepatol.* 8, 166 (**2009**).

24. W. Z. Kolozsi, Y. El.Gohary, E. B. Keeffe, and J. F. Rossignol, *Am. J. Gastroenterol.* 103, S150 (**2008**).

25. M. Elazar, M. Liu, S. McKenna, P. Liu, E. A. Gehrig, A. Elfert, J. Puglisi, J. F. Rossignol, and J. S. Glenn, *Hepatol.* 48, 1151A (**2008**).

26. M. Clerici, D. Trabattoni, M. Pacei, M. Biasin, and J. F. Rossignol, *J. Immunol.* 186, 155 (**2011**).

27. J. R. Murphy and J. C. Friedmann, *J. Appl. Toxicol.* 5, 49 (**1985**).

28. K. Kataoka, A. Harada, and Y. Nagasaki, *Adv. Drug Del. Rev.* 47, 113 (**2001**).

29. S. R. Croy and G. S. Kwon, *Curr. Pharm. Design* 12, 4669 (**2006**).

30. A. Sosnik, A. Carcaboso, and D. A. Chiappetta, *Recent Pat. Biomed. Eng.* 1, 43 (**2008**).

31. D. A. Chiappetta and A. Sosnik, *Eur. J. Pharm. Biopharm.* 66, 303 (**2007**).

32. A. Sosnik, C. Alvarez-Lorenzo, and A. Concheiro (Eds.), Royal Society of Chemistry, London, In press.

33. J. Gonzalez-Lopez, C. Alvarez-Lorenzo, P. Taboada, A. Sosnik, I. Sandez-Macho, and A. Concheiro, *Langmuir* 24, 10688 (**2008**).

34. D. A. Chiappetta, J. Degrossi, S. Teves, M. D'Aquino, C. Bregni, and A. Sosnik, *Eur. J. Pharm. Biopharm.* 69, 535 (**2008**).

35. D. A. Chiappetta, C. Hocht, C. Taira, and A. Sosnik, *Nanomedicine (Lond).* 5, 11 (**2010**).

36. D. A. Chiappetta, C. Hocht, C. Taira, and A. Sosnik, *Biomaterials* 32, 2379 (**2011**).

37. R. N. Peroni, S. S. Di Gennaro, C. Hocht, D. A. Chiappetta, M. C. Rubio, A. Sosnik, and G. F. Bramuglia, *Biochem. Pharmacol.* 82, 1227 (**2011**).

38. A. Ribeiro, A. Sosnik, D. A. Chiappetta, F. Veiga, A. Concheiro, and C. Alvarez-Lorenzo, *J. Royal Soc.-Interface* 9, 2059 (**2012**).

39. D. A. Chiappetta, C. Hocht, J. A. W. Opezzo, and A. Sosnik, *Nanomedicine (Lond.)* 8, 223 (**2013**).

40. M. L. Cuestas, A. Castillo, A. Sosnik, and V. L. Mathet, *Bioorg. Med. Chem. Lett.* 22, 6577 (**2012**).

41. C. Alvarez-Lorenzo, A. Rey-Rico, J. Brea, M. I. Loza, A. Concheiro, and A. Sosnik, *Nanomedicine (Lond.)* 5, 1371 (**2010**).

42. M. L. Cuestas, A. Sosnik, and V. L. Mathet, *Mol. Pharmaceutics* 8, 1152 (**2011**).

43. A. Sosnik, *Adv. Drug Del. Rev.* in preparation.

44. C. Eisenburg, N. Seta, M. Appel, G. Feldmann, G. Durand, and J. J. Feger, *Hepatol.* 13, 305 (**1991**).

45. L. Fiume, C. Busi, G. Di Stefano, and A. Mattioli, *Adv. Drug Del. Rev.* 14, 51 (**1994**).

46. Y. Li, G. Huang, J. Diakur, and Ll. Wiebe, *Curr. Drug Deliv.* 5, 299 (**2008**).

47. R. Kikker, B. Lepenies, A. Dibekian, P. Laurino, and P. H. Seeberger, *J. Am. Chem. Soc.* 131, 2110 (**2009**).

48. J. Zhang, C. Li, Xue-ZY, H. W. Cheng, F. W. Huang, R. X. Zhuo, and X. Z. Zhang, *Acta Biomater.* 7, 1655 (**2011**).

49. M. L. Cuestas, R. J. Glisoni, V. L. Mathet, and A. Sosnik, *J. Nanopart. Res.* 15, Art. 1389 (**2013**).

50. F. P. Bruno, M. R. Caira, G. A. Monti, D. E. Kassuha, and N. R. Sperandeo, *J. Mol. Struct.* 984, 51 (**2010**).

51. D. A. Chiappetta, G. Facorro, E. Rubin de Celis, and A. Sosnik, *Nanomedicine: NBM* 7, 624 (**2011**).

52. J. Dong, B. Z. Chowdhry, and S. A. Leharne, *Colloids Surf. A: Physicochemical and Engineering Aspects* 212, 9 (**2003**).

53. A. V. Kabanov, I. R. Nazarova, I. V. Astafieva, E. V. Batrakova, V. Y. Alakhov, A. A. Yaroslavov, and V. A. Kabanov, *Macromolecules* 28, 2303 (**1995**).

54. L. Wan, X. Zhang, S. Pooyan, M. S. Palombo, M. J. Leibowitz, S. Stein, and P. J. Sinko, *Bioconj. Chem.* 19, 28 (**2008**).

55. D. A. Chiappetta, J. Degrossi, R. A. Lizarazo, D. L. Salinas, F. Martínez, A. Sosnik, L. Segewicz, and M. Petrowsky (eds.), Nova Publishers, Hauppauge, NY (**2011**), p. 197.

RESEARCH ARTICLE